Implications of orthopedic fretting corrosion particles on skeletal muscle microcirculation

C. N. KRAFT[1]*, B. BURIAN[1], O. DIEDRICH[1], M. A. WIMMER[2]
[1]*Department of Orthopaedic Surgery, Rheinische Friedrich-Wilhelms-University, D-53105 Bonn, Germany*
[2]*AO-Research Institute, Clavadelerstrasse, CH-7270 Davos, Switzerland*
Email: umcb01@uni-bonn.de

Particulate corrosion and wear products of metal implants are increasingly becoming topics of interest, due to the cascade of biological and biomechanical events they induce. The impairment of skeletal muscle microcirculation by fretting corrosion particles may have profound consequences. We therefore studied *in vivo* leukocyte–endothelial cell interaction in skeletal muscle after confrontation with characterized titanium and stainless steel fretting corrosion particles, and compared these results with those of the bulk materials. Using the hamster dorsal skinfold chamber preparation and intravital microscopy, we could demonstrate that stainless steel induces a more pronounced inflammatory answer in contrast to the implant material titanium. However, we were not able to show a general benefit of bulk vs. debris. Overall, the study suggests that not only the bulk properties of orthopaedic implants, but also the microcirculatory implications of inevitable wear debris, may play a role in determining biocompatibility and ultimately longevity of an implant. The skinfold chamber is a feasible and versatile model for observation of the dynamic process of microvascular response after foreign-body implantation, and offers much perspective.

1. Introduction

Wear particles are produced from the articulating and non-articulating surfaces of artificial devices and accumulate in tissues in the vicinity of the implant [1–5]. Numerous studies have shown that particulate debris is not biologically inert and tissue responses have directly been related to corrosion products, of and wear debris from metal orthopedic implants [5–7]. In this context it has been postulated that metallic wear may induce a cascade of inflammatory events, that ultimately result in bone loss by osteolysis and subsequent implant failure in the form of aseptic loosening or even corrosion-related fracture [5, 8, 9]. Though it is recognized that the host's chronic response is related to the type and size of particulate wear [10], the duration of exposure [11, 12] and the surface characteristics [13], little is known about the acute implications of wear debris on soft tissue. Taking into consideration that a long bone's nutrition is substantially dependent on the integrity of the surrounding soft tissue, and here primarily of the adjacent striated muscle [14, 15], impairment of the muscles microcirculation may have profound consequences for osseous tissue. Bone necrosis may be facilitated, and in cases where foreign body implants have been inserted, osseous integration may be impeded or early implant loosening observed. The purpose of this study was to describe a new *in vivo* model and to elucidate the effects of titanium and stainless steel wear debris on the leukocytic response in skeletal muscle. These results were compared with those of bulk implants of the same material.

2. Materials and methods

2.1. Animal model

For our study we used Syrian golden hamsters (*Mesocricetus auratus* 6–8 weeks old, 60–80 g body wt), kept on standard pellet food and water *ad libitum*. For *in vivo* fluorescence microscopy a dorsal skinfold chamber [16], containing striated muscle and skin and allowing for repeated analysis of the microcirculation in the awake animal over a prolonged period of time, was implanted under pentobarbital sodium anesthesia (50 mg/kg body wt ip). The animals were fitted with two symmetrical titanium frames, positioned on the dorsal skinfold, sandwiching the extended double layer of skin. One layer of skin was completely removed in a circular area of 15 mm in diameter, and the remaining layers (consisting of striated muscle and subcutaneous tissue and skin) were covered with a removable cover slip, incorporated into one of the titanium frames. Fine polyethylene catheters were inserted into the jugular

* Author to whom correspondence should be addressed, at Department of Orthopaedic Surgery, University of Bonn, Sigmund Freud-Str. 25, 53127 Bonn.

vein. A recovery period of 72 h between surgery and start of the experiments was allowed to eliminate the effects of anesthesia and microsurgery on the microvasculature.

2.2. Bulk implants

Large samples (4 mm^3) large with a thickness of 0.5 mm consisting of either stainless steel (SSt) or commercially pure titanium (Ti) were used. The steel and titanium implants were made of the identical material as used in plates widely utilized in plate osteosynthesis according to ISO 5832-1 and ISO 5832-2 respectively. Their chemical composition (in weight-%) was as follows: Stainless steel: 17.66% Cr, 14.29% Ni, 2.81% Mo, 1.74% Mn, 0.088% N, 0.040% Cu, 0.027% C, 0.018% P, 0.014% Si, 0.001% S, balance ($>$ 63.3%) Fe; cp titanium: 0.3% O, 0.01% C, 0.02% Fe, 0.006% N, balance ($>$ 99.6%) Ti. The implants were specifically produced and kindly supplied by the Dr Robert Mathys Foundation, Switzerland.

2.3. Particulate wear

The fretting wear particles were produced from the same materials as the plates. The ''fretting wear simulator'' consists of a laboratory stirrer and a Teflon® coated ''following head''. The following head is studded on the underside with pins of commercially pure titanium or stainless steel of implant quality, then placed in a beaker to the bottom of which a disc of the same metal is attached. Ringer solution is used as lubricant and the beaker is sealed with cling film. Fretting particles are generated due to the specific motion characteristics of the following head: wobbling of the stirring head (because of hydrodynamic effects) causes stick-slip movement between pins and disk. The particles are extracted from the media by means of ultra-centrifugation. The slag obtained is dried at 50 °C and pulverized using a mortar afterwards. The particles were heat-sterilized for 3 h at 180 °C and filled into a ∅2.2 mm tube, which is locked with a piston at one end. After slight compaction, the height of the titanium and steel particles inside the tube was adjusted to 0.5 mm each, thus controlling for equal wear volume. In addition, the weight was controlled using a balance with a nominal precision of 0.01 mg (AT261 DeltaRange, Mettler Toledo, Greifensee, Switzerland). After filling, the other end of the tube was also closed, and the whole device gamma-sterilized after packaging.

The generated particles were described according to their size and shape using scanning electron microscopy in the backscattered mode. A detailed description of the method is given by ap Gwynn and Wilson [17]. Briefly, the heat sterilized particles were put into acetone at a concentration of approx. 0.1 mg/ml and thoroughly mixed using ultra-sound and a mechanical shaker. Then a drop of the solution was placed on a SEM specimen stub covered with Thermanox-film. After drying of the specimens under clean air, samples (five each) were coated with an 8.8 nm carbon layer and the edges of the stub were painted with Ag-enamel in order to improve the electrical conductivity of the sample. Fifty images each of titanium and stainless steel particles were taken in the backscattered mode at 5 kV acceleration voltage. For later calibration using image analysis software, also latex particles of known size and shape (spheres of 10 μm) were recorded. A total of 993 SSt- and 643 Ti-particles were subjected to measurements using a computer-program (PC-Image VGA24, version 2.2.03). The area and the perimeter of the particles were measured. To describe particle size, the ''equivalent circle diameter'' (ECD) was plotted, which is the diameter of a circle that has the same area as the analyzed particle. For particle shape ''circularity'' was chosen, which is a measure derived from the equation $4 \times \text{area}/(\text{perimeter})^2$. The circularity can range from 0 (needle-shaped) to 1 (perfectly round). Descriptive statistical analysis and linear regression analysis of the measures was performed.

To study the composition of the generated debris X-ray diffraction analysis was performed using a D5000 Theta–Theta Diffractometer (Siemens, Germany) equipped with a copper tube. Heat sterilized particles were fixed on glass using hair spray and analyzed at 40 kV and 40 mA in the range of 2–100° 2-Theta. The diffractometer readings were corrected for noise, which was generated due to the glass specimen holder.

2.4. Implantation technique

Implants/wear debris were brought into position by removing the cover slip of the titanium frame and placing the corrosion products/metal plate directly onto the striated muscle and subcutaneous tissue. Implant thickness was chosen in such a way, so as not to mechanically irritate or impede microcirculation after replacement of the cover slip. No further manipulation of the skinfold chamber occurred after this initial implantation.

2.5. Experimental groups

Animals were randomly assigned to the following five groups: commercially pure titanium wear debris (Ti-wear; $n = 6$), implant quality stainless steel wear debris (SSt-wear; $n = 6$), commercially pure bulk titanium (Ti-bulk; $n = 6$), implant quality bulk stainless steel (SSt-bulk; $n = 6$), controls (Cntrl.; no implant, $n = 6$).

2.6. Intravital fluorescence microscopy and microcirculatory analysis

For *in vivo* microscopic observation, the awake animals were immobilized in a Plexiglass tube, and the skinfold preparation was attached to the microscope stage. By use of a modified Leica DM-LM-D microscope with a 100-W HBO mercury lamp, attached to a LU 4/25 fluorescence illuminator with an I3 blue and N2.1 green filter block (Leica Microsystems, Bensheim, Germany) for epi-illumination, the microcirculation was recorded by means of a charge-coupled device video camera and images were transferred to a video system for frame-by-frame off-line quantification [18]. Leukocytes were stained *in vivo* with rhodamine-6G (0.1 μmol/kg) and classified according to their interaction with the vascular

endothelial lining as adherent, rolling or free flowing cells. Adherent leukocytes were defined in each vessel segment as cells that did not move or detach from the endothelial lining within a specified observation period of 20 s and are given as number of cells per mm squared of endothelial surface, calculated from diameter and length of the vessel segment studied, assuming a cylindrical geometry. Rolling leukocytes were defined as those white blood cells moving at a velocity less than two-fifths of the center-line velocity and are given as percentage of nonadherent leukocytes passing through the observed vessel segment within 20 s. Baseline measurements were performed immediately after intravenous injection of the fluorescent marker and subsequently after 30 min, 120 min, 8 h, 24 h, 3, 7 and 14 days after plate/particle implantation.

2.7. Experimental protocol

Baseline recordings for analysis of leukocyte-endothelial cell interaction and assessment of microvascular permeability included approximately 8–10 individual postcapillary and collecting venules. After baseline recording, the plates/particles were implanted, taking care to avoid contamination, mechanical irritation or damage to the chamber. Microcirculatory analyzes were repeated at 30 min, 120 min, 8 h, 24 h, 3, 7 and 14 days after implantation. In control animals identical frames were video-documented, thus allowing assessment of identical vessels throughout the experiment. In experiments with implants we could not exclude that individual blood vessels selected for microscopic study at baseline were covered by the implanted material, thus requiring selection of microvessels for microscopic study different from those analyzed at baseline. However, identical microvessels could then be studied at time points 30 min, 120 min, 8 h, 24 h, 3, 7 and 14 days after implantation.

2.8. Statistical analysis

The statistical procedure included analysis of variance and Student's t test for comparison between the groups. Paired Student's t test was performed for analyzing differences within each group. Values are reported as means $\pm$ SEM, and the level of statistical significance was set at $p < 0.05$.

3. Results

3.1. Wear debris

The production rate for wear particles differed between Ti and SSt. The same particle volume was generated 23-times faster when Ti was worn. Per beaker and day 114 mg vs. 4.95 mg wear debris was generated (for Ti re. SSt). The generated Ti-particles were bigger in size, having an ECD of 0.64 ± 0.77 µm (range: 0.09–7.79 µm), whereby 95% were smaller than 2 µm. Their circularity was 0.62 ± 0.16. Most of the evaluated SSt-particles were smaller in size with an ECD of 0.17 ± 0.37 µm, whereby the size deviation ranged from 0.06–6.2 µm). 95% of the investigated particles were smaller than 0.5 µm. The circularity of SSt was comparable to Ti: 0.57 ± 0.19. Figs 1A and B show a frequency plot of both types of fretting particles. Note that the non-symmetric character of the size distribution with its maximum occurring at 80 nm for SSt particles. Ti in contrast displays its maximum at 200 nm. As shown by the circularity plotted per class, there is a slight, yet not significant, decrease of the circularity with increasing ECD for both materials.

Diffraction patterns for Ti displayed mostly metallic titanium, and secondary titanium oxides with changing stochiometry. Beside the reflection peak for FeCrNi-steel, SSt showed in addition reflections for chromium–nickel-oxides. For both materials, Ti and SSt, the crystal peaks were superimposed by a considerable amorphous fraction.

3.2. Intravital microscopy

3.2.1 General characteristics

Thirty-three animals were treated, of which 30 were finally evaluated. Three animals died due to complications associated with the anesthesia during initial fitting of the dorsal skinfold chamber. Implantation of the metal plate or wear debris was tolerated well by the animals. In the group treated with stainless steel wear debris evaluation of all microvascular parameters was only possible up until 8 h after implantation. Massive oedema of the tissue under investigation impeded further assessment.

3.2.2 Leukocyte–endothelial cell interaction

Under baseline conditions most leukocytes did not interact with the endothelial surface of the microvessels under study, although there was a fraction of, in some cases $\sim$ 10–20%, white blood cells showing spontaneous rolling along the endothelial lining of postcapillary and collecting venules. In all groups implantation of bulk and wear products led to an activation of leukocytes with a notable increase of the leukocyte–endothelial cell interaction within the first 30 min, compared to controls. This initial increase of rolling and adherent leukocytes was found to be transient in the Ti-plate after 24 h, and in the Ti-wear group after 3 days (Figs 2A and B). SSt-plates and -wear induced a massive significant inflammatory response within the first 8 h after implantation (adherent leukocytes (n/mm2): Ti-plate BL: 30.04 ± 3.75 vs. 8 h: 202.68 ± 20.53; Ti-wear BL: 35.16 ± 11.07 vs. 8 h: 226.00 ± 37.66; SSt-plate BL: 40.58 ± 2.72 vs. 8 h: 827.82 ± 167.92; SSt-wear BL: 48.31 ± 14.59 vs. 8 h: 753.21 ± 3.96) After 8 h, the animals treated with bulk SSt-implants showed signs of recuperation, though venular leukocyte rolling remained persistently high in this group throughout the ensuing observation periods, compared to Ti-bulk, Ti-wear and controls (Fig. 2A). Interestingly, when compared to all other implant groups, we found diminished leukocyte rolling between 30 min and 120 min after SSt-wear implantation despite persistingly high leukocyte adherence in the same observation period. Further evaluation of leukocyte–endothelial cell interaction in all animals treated with SSt-debris was not possible later than 8 h due

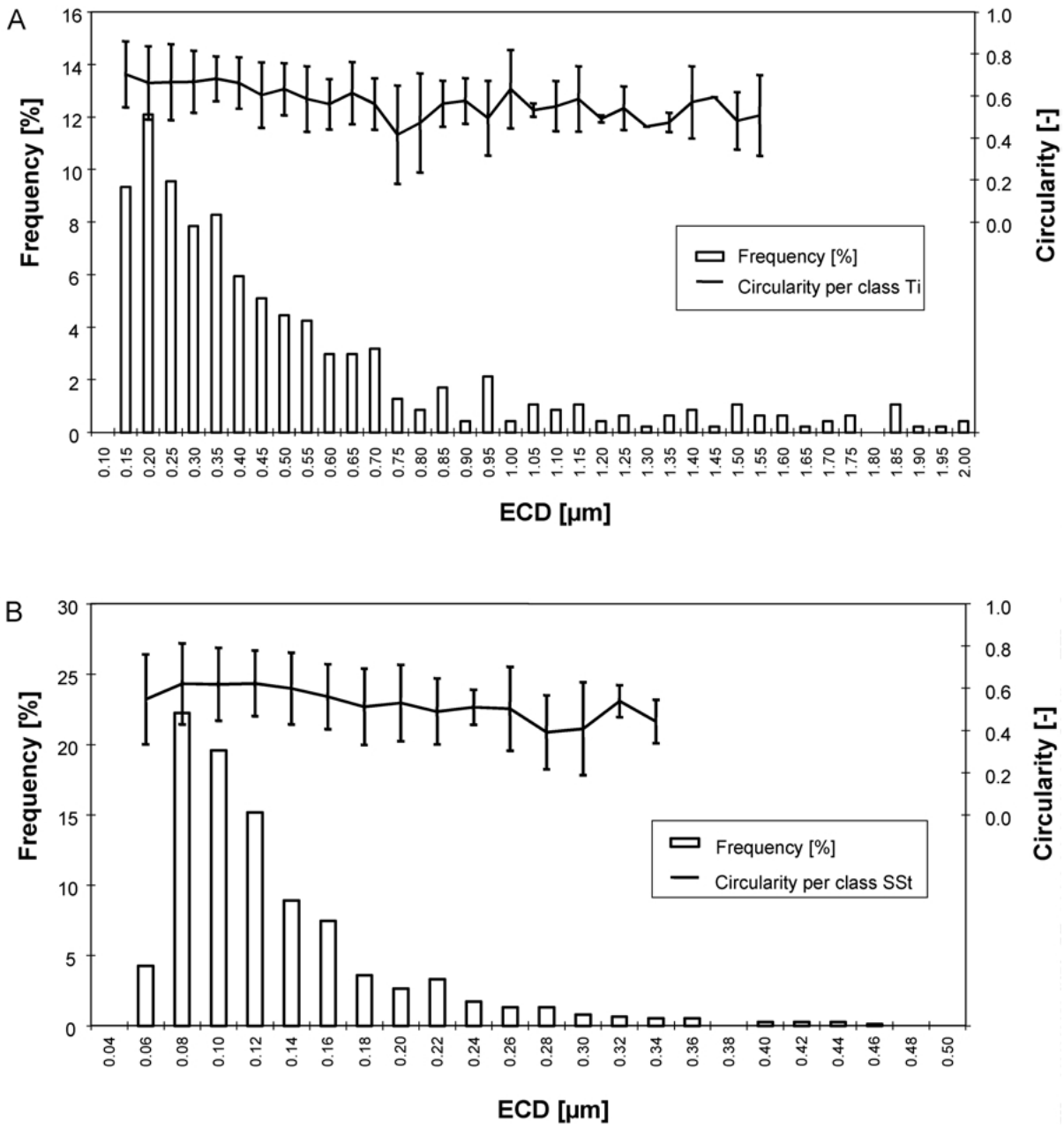

Figure 1 Frequency distribution of the equivalent circle diameter of titanium (A) and stainless steel (B) wear debris. Note that in both cases 95% of the whole particle fraction is shown. 5% of the remaining titanium particles ranged from 2 to 7.1 µm, whereby not shown stainless steel particles displayed values between 0.5 and 6.2 µm. Due to the different size ranges of both particle fractions, classes do not match. For classes with more than six particles the circularity is plotted as mean $\pm$ S.D.

to massive inflammation and edema of the skinfold chamber (Figs 2A and 2B).

4. Discussion

There are numerous papers studying the biological effects of particulate debris on host tissue or cells, whereby less attention has been focused on particles generated by fretting or fretting corrosion [19]. In this study we tried to replicate wear which may occur between the screw head and the plate for osteosynthesis. Cells respond to the physical presence of particles, in addition to any chemical products that arise from the particles' exposure to the physiological environment. In that, fretting particles may differ from bulk implants, because their composition can deviate due to tribochemical reactions and/or chemical attack (corrosion). Although all generated Ti and SSt particles were not completely oxidized, partially showing amorphous structure, the chromium–nickel-oxide layer for SSt-particles differs from the chromium oxide layer of bulk implants. It needs further analysis, whether nickel in this oxide layer is bound as NiO_x or occurs as free Ni^0. If the latter is true, it will go quickly into solution as Ni^{2+}. According to an extensive review article from Savio *et al*. [20], Ti wear particles were frequently observed *in vivo*. Some investigators report Ti wear particles less than 1 µm, others in the 1–5 µm size range. Sub-micron SSt particles are also identified quite often, however, SSt particles in the 1–5 µm range are more commonly reported. Urban *et al*. [21], reported in a recent article of disseminated wear to organs and lymph nodes, that

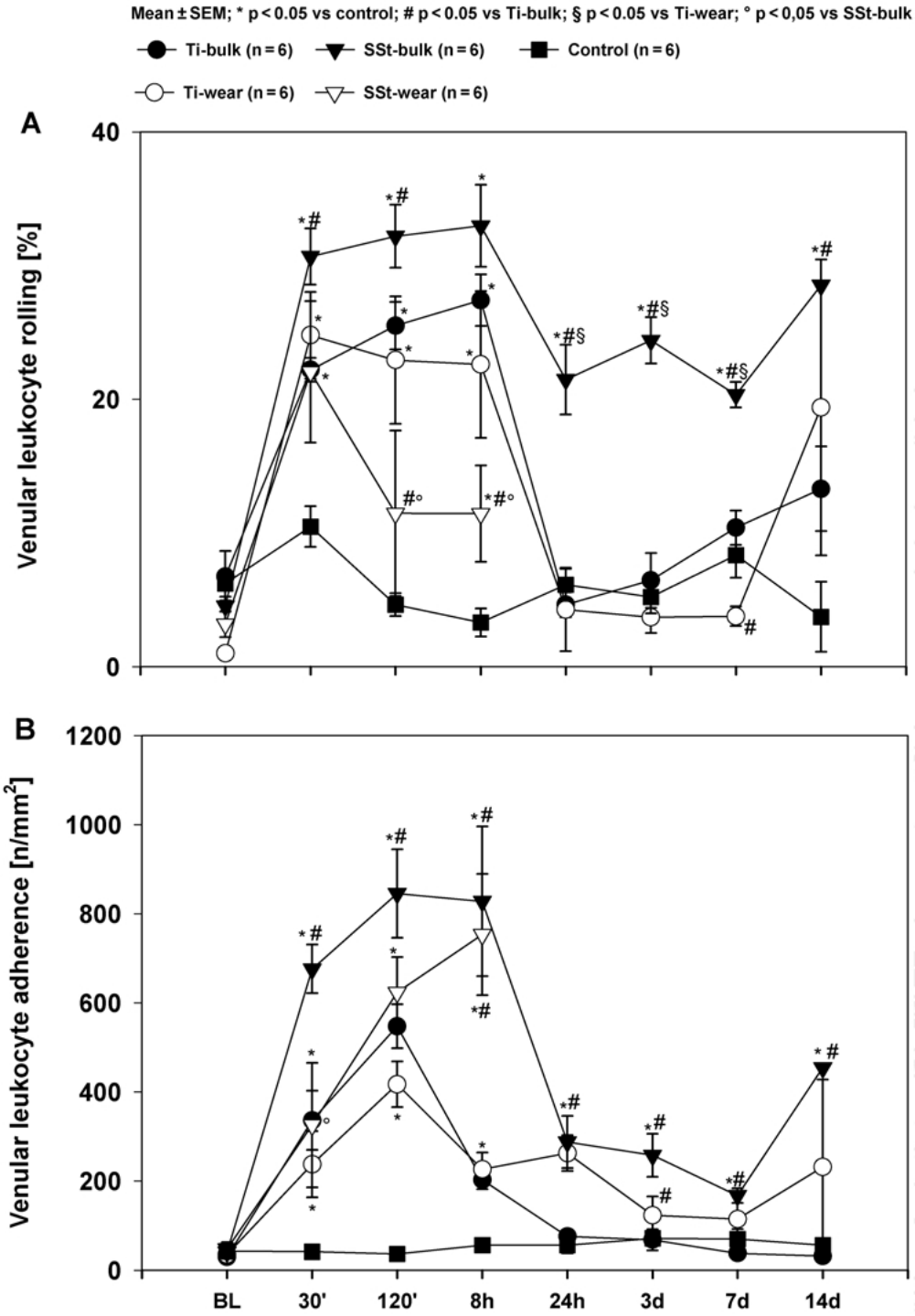

Figure 2 (A) Number of rolling leukocytes (given in % of non-adherent leukocytes) and (B) number of firmly adherent leukocytes (number of cells/mm^2 endothelial surface) in postcapillary and collecting venules of striated muscle in the hamster dorsal skinfold preparation before (BL, baseline) and 30 and 120 min as well as 8 h, 24 h, 3, 7 and 14 days after implantation of debris/plates. Means ± SEM. Unpaired Student's *t*-test for comparison between groups with $P < 0.05$ * vs. control, # vs. Ti-bulk, § vs. Ti-wear, ° vs. SSt-bulk.

most of the Ti and SSt wear debris was smaller than 1 μm, ranging from as low as 0.1 μm up to 50 μm for Ti, whereby SSt rarely exceeded 3 μm. Although, there is very little information regarding the shape and composition of *in vivo* wear debris, the applied particle fraction, at least size-wise, seems to replicate *in vivo* wear debris fairly well.

Cell/particle interactions have been predominantly studied using *in vitro* set-ups. Our model is unique in that leukocyte response in the vicinity of metal debris is studied *in vivo*. This model allows for the observation and quantification of the dynamic processes of host versus particulate debris. Prior experiments [22] have demonstrated that the dorsal skinfold chamber model can be standardized and enables the *in vivo* analysis of leukocyte flow behavior, delivering quantitative data on numerous parameters derived from the confrontation of the host organism with an implant.

We could demonstrate that stainless steel induces a more pronounced inflammatory answer in contrast to the implant material titanium. This is in unison with older literature, where Ti was found to be more biocompatible compared to SSt [23, 24]. However, we were not able to show a general benefit of bulk versus debris. Titanium

wear debris induced a slightly more pronounced inflammatory reaction than its bulk product, especially concerning the extravasation of leukocytes. SSt-wear debris, although initially slightly less inflammatory, had a more marked and persisting negative effect on leukocyte–endothelium interaction compared to its bulk product. The host's inflammatory response increased to such an extent that ultimately microcirculation broke down within 24 h after particle implantation in all treated animals. Our observations may be explained by constituents of stainless steel, which are capable of eliciting highly cytotoxic reactions and inducing an immunological response within the host, namely chromium [25, 26] and nickel [27]. Nickel and chromium ion release may explain the massive edema and parenchymal injury observed in the group treated with stainless steel wear debris, and to a reduced amount in those treated with stainless steel implants. This discrepancy may most likely be explained by occurrence of free nickel (and chromium) within the oxide layer of the SSt particles. In addition, the enlarged surface area of the debris as a whole, as well as the increased tissue–metal contact-area in debris treated animals, may play a role. The clinical implications regarding the effects that chemical dissolutes and wear products from stainless steel implants have on biological tissue have frequently been discussed. In the clinical situation, peri-implant fluids contain significant amounts of both particulate and soluble metal [28]. Particularly in orthopedic implant conditions, localized mechanical stress or fretting may damage the passivating oxide layer, cause an increase in corrosion and release of wear particles. It has been shown, that the release of ions and particulate debris of all orthopedic metallic alloys has the capability of eliciting a significant alarming response, and toxicity profiles have been established, placing nickel and chromium ions among the most damaging metal ions [25, 26, 29].

While these results are alarming, it should be considered that the same wear volume is generated much faster with titanium implants than it is with stainless steel implants. Overall, the study suggests that not only the bulk properties of orthopedic implants but also the composition, size and shape of inevitable wear debris on the local microcirculatory system may play a pivotal role in determining long-term biocompatibility. What precise effect particle size, shape and particle composition with possible further degradation have on the microvascular perfusion remain to be analyzed. With a minimum of adverse host reaction, our results indicate that titanium still represents the gold standard in metallic implant material, even in the case of generated wear debris, which shows a comparatively low inflammatory potential.

Acknowledgments

The study was financed in part by AO/ASIF; Research Grant Nr. 2000-K78. The bulk implants used in this study were kindly supplied by the Robert Mathys Foundation, Bettlach, Switzerland. The diffraction analyzes were performed by Dr Martin Sulkowski, University of Essen. The authors wish to thank Mr Werner Masson, member of the technical staff of the Orthopaedic Research Unit, Rheinische Friedrich-Wilhelms University of Bonn, and Ch. Sprecher, technical engineer of the AO Research staff for their co-operation and assistance in this study.

References

1. H. J. AGINS, N. W. ALCOCK, M. BANSAL, E. A. SALVATI, P. D. WILSON JR, P. M. PELLICCI and P. G. BULLOUGH, *J. Bone Joint Surg.* **70A** (1988) 347.
2. J. BLACK, H. SHERK, J. BONINO, W. R. ROSTOKER, F. SCHAJOWICZ and J. O. GALANTE, *ibid.* **72A** (1990) 126.
3. L. D. DORR, R. BLOEBAUM, J. EMMANUAL and R. MELDRUM, *Clin. Orthop.* **261** (1990) 82
4. C. P. CASE, V. G. LANGKAMER, C. JAMES, M. R. PALMER, A. J. KEMP, P. F. HEAP and L. SOLOMON, *J. Bone Joint Surg.* **76B** (1994) 701.
5. J. J. JACOBS, J. L. GILBERT and R. M. URBAN, *ibid.* **80A** (1998) 268.
6. D. F. WILLIAMS and G. MEACHIM, *J. Biomed. Mater. Res.* **8** (1974) 1.
7. R. M. URBAN, J. J. JACOBS, J. L. GILBERT and J. O. GALANTE, *J. Bone Joint Surg.* **76A** (1994) 1345.
8. J. R. MORELAND, *Clin. Orthop. Rel. Res.* **226** (1988) 49.
9. T. T. GLANT and J. J. JACOBS, *J. Orthop. Res.* **12** (1994) 720.
10. J.-M. LEE, E. A. SALVATI, F. BETTS, E. F. DICARLO, S. B. DOTY and P. G. BULLOUGH, *J. Bone Joint Surg.* **74B** (1992) 380.
11. H. G. WILLERT and M. SEMLITSCH, *J. Biomed. Mater. Res.* **11** (1977) 157.
12. D. W. HOWIE, *J. Arthroplasty* **5** (1990) 337.
13. J. D. WITT and M. SWANN, *J. Bone Joint Surg.* **73(B)** (1991) 559.
14. J. K. MCGEACHIE and M. D. GROUNDS, *Cell Tissue Res.* **248** (1987) 125.
15. C. KRETTEK, *Chirurg* **69** (1998) 684.
16. B. ENDRICH, K. ASAISHI, A. GÖTZ and K. MESSMER, *Res. Exp. Med.* **177** (1980) 125.
17. I. AP GWYNN and C. WILSON, *Eur. Cells Mat.* **1** (2001) 1.
18. A. R. PRIES, *Int. J. Microcirc. Clin. Exp.* **7** (1988) 327.
19. J. J. JACOBS, S. B. GOODMAN, D. R. SUMNER and N. J. HALLAB, in ''Orthopaedic Basic Science'' (American Academy of Orthopaedic Surgeons, Rosemont, 2000) p. 402.
20. J. A. SAVIO, L. M. OVERCAMP and J. BLACK, *Clin. Mater.* **15** (1994) 101.
21. R. M. URBAN, J. J. JACOBS, M. J. TOMLINSON, J. GAVRILOVIC, J. BLACK and M. PEOC'H, *J. Bone Joint Surg.* **82A** (2000) 457.
22. C. N. KRAFT, M. HANSIS, S. ARENS, M. D. MENGER and B. VOLLMAR, *J. Biomed. Mater. Res.* **49** (2000) 192.
23. U. N. RIEDE, T. P. RÜEDI and F. LIMBACHER, *Arch. Orthop. Unfall-Chir.* **79** (1974) 205.
24. T. P. RÜEDI, *Unfallchirurgie* **123** (1975) 1.
25. K. MERRITT and S. BROWN, *Clin. Orthop.* **329** (1996) 233.
26. M. G. SHETTLEMORE and K. J. BUNDY, *J. Biomed. Mater. Res.* **45** (1999) 395.
27. M. UO, F. WATARI, A. YOKOYAMA, H. MATSUNO and T. KAWASAKI, *Biomaterials* **20** (1999) 747.
28. Z. L. SUN, C. WATAHA and C. T. HANKS, *J. Biomed. Mater. Res.* **34** (1997) 29.
29. J. O. GALANTE, J. LEMONS, M. SPECTOR, P. D. WILSON and T. M. WRIGHT, *J. Orthop. Res.* **9** (1991) 760.

Received 14 May
and accepted 30 May 2001